

RESEARCH ON SOLUTION STRENGTHENED FERRITIC DUCTILE IRON (SSFDI) STRUCTURE AND PROPERTIES USING DIFFERENT TREATMENT AND INOCULATION MATERIALS

C. Hartung, Eivind G. Hoel, and Emmanuelle Ott
ELKEM Foundry Products Division, Ålvik, Norway

R. Logan
ELKEM Metals Inc, Coraopolis, USA

Andy Plowman and David Wilkinson
ELKEM Limited, Sheffield, UK

Copyright © 2020 American Foundry Society
<https://doi.org/10.1007/s40962-020-00469-4>

Abstract

A market review of solution strengthened ferritic ductile iron (SSFDI or SSF) is provided as a backdrop for research work conducted by Elkem over the past 5 years. This research included trials that were specifically designed and conducted on SSF materials to better understand how these irons behave when varying magnesium ferrosilicon (MgFeSi) and inoculating materials are used. During this research, three extensive trials were conducted during which 20 treatment ladles were made to study the effect of five different MgFeSi alloys, nine different types of inoculants, and two cover materials. In addition, the influence of separate antimony (Sb) additions

made during inoculation was tested to see if this element enhanced the structure and reduced the risk of forming chunky graphite. The results of this research demonstrated the effect of these variations on the thermal analysis, microstructure, mechanical properties, and shrinkage tendency with emphasis on some of the differences between regular and SSF ductile irons.

Keywords: ductile irons, solution strengthened ferritic irons, solid solution, strengthening mechanisms, casting, cover materials, MgFeSi, inoculants, antimony, bismuth

Introduction

Early SSF Developments

Both academic research and industrial research are continually developing new materials having improved properties and lower weights without compromising design integrity or service reliability. In fact, lightweight designs are central to improving efficiency and optimizing energy consumption. For these reasons, it is imperative that

enhanced materials are continuously researched and developed to meet these demands.

Much of this interest has been focused on various generations of high-silicon ductile iron that were originally published in Swedish standards and subsequently by EN 1563:2011. These grades are also known as ferritic-pearlitic and solution strengthened ferritic (SSF) ductile iron. These SSF grades contain elevated levels of Si, typically between 3 and 4.5%. They are particularly important because of their inherent capability to cast complex shapes that provide excellent mechanical properties at relatively low cost. The use of these iron grades was initially studied by Volvo in the early 1980 s.

This paper is an invited submission to IJMC selected from presentations at the 6th Keith Millis on Ductile Iron held October 23–26, 2018, at the Sonesta Resort, Hilton Head Island, SC. It is published in the IJMC by permission of the DIS (Ductile Iron Society).

Within the ferritic/pearlitic DI grades, varying cooling rates normally caused by different section thicknesses promote differing levels of pearlite and very different microstructures. These structural changes create significantly greater variations in hardness and mechanical properties than are found in a purely ferritic structure. The development of the SSF grades has provided a solution to this challenge, allowing for greater market penetration with the potential for increasing usage in different engineering applications.

Over the years, various conferences and Keith Millis Symposiums have featured technical papers and developments about SSF iron. One of the early publications presented at the 2003 Keith Millis, claiming that ductile iron alloyed with high levels of Si had “excellent ductility and machinability”,¹ was written prior to the SSF nomenclature and EN 1563 revisions that included these new grades. This paper highlighted some of the work done by Volvo that showed that SSF iron gave improvements in machinability compared to grade 500-7 baseline and traditional iron grades having the same tensile strength and similar hardness.

At the 2008 Keith Millis, Larker discussed the application of this higher Si iron in new parts, the tremendous reduction in hardness variation, and the benefits of avoiding pearlite in the microstructure.²

Charpy Testing

One of the concerns with SSF iron has been impact properties, particularly at low temperatures. These properties have been measured using a Charpy impact tester that measures impact property energy data for both notched and unnotched sections. This test is also used to identify the ductile-to-brittle transition temperature of a material. The Charpy test was developed in the early 1900 s, but was most beneficial when determining the steel failure mechanism of cracks in liberty ships during World War II. At a DIS seminar in 2011, a paper discussed the relevance of the Charpy test and data used for design and engineering of parts and components.³ This paper recommended that better methods of measuring impact toughness, particularly for iron, should be considered.

At the 2013 Keith Millis, Stets⁴ introduced the revised standard EN 1563 and shared some interesting and groundbreaking work. This revised standard includes a new family of high-Si, ductile iron grades, also known as SSF grades, having enhanced properties. It is interesting that while the EN1563 includes a minimum impact requirement, it only specifies unnotched room-temperature testing. The absence of low-temperature impact properties downplays the importance of using traditional test methods to guide impact properties and toughness.

New Applications

Also, of major significance within the past decade is the fact that manufacturers of large windmills have started to develop and specify SSF iron for very heavy-sectioned, ductile iron casting designs to improve material consistency and reduce the weight of components. Furthermore, work published in 2014 by Componenta Döküm, a large Finnish engineering company, again highlighted the many advantages of SSF iron and its growing use in many parts.⁵ In addition, today’s designers have started to appreciate that the stress/strain conditions of the impact test are orders of magnitude different than shown by traditional Charpy testing. As a result, the Charpy impact test is not suitable in simulating real-world impact conditions.

Recent research has focused on the optimization of SSF chemistry, and more is expected in the future. Studies in 2015 showed that EN-GJS-600-10 SSF iron had an improved graphite structure and properties with additions of between 2 and 4% cobalt (Co).⁶ In June 2016, a DIS Research Committee initiative presented the results of a 9-question survey on SSF iron grades. The clear majority of the survey responders agreed that more research should be done on SSF iron in three main categories: (a) fatigue and other properties, (b) increased propensity towards porosity, and (c) graphite structure control.⁷ Recently, research has studied the variation in tensile properties of SSF iron, focusing on the chemical composition.⁸ An additional investigation is proposed by a DIS research project that will investigate the effects of residual alloying elements.⁹

SSF Iron Market Analysis

Because of the growing interest and expanding use of SSF iron during the past few decades, the current and future global market for SSF iron was examined.¹¹ According to the most recent production figures, the total annual global production of ductile iron was 25,467,378 tons in 2016.¹⁰ Recently, some growth has been seen in the use of pearlitic ductile iron grades, EN-GJS 500-7 and EN-GJS 600-3, which have transitioned to SSF iron; however, the largest interest and investment seems to be in the EN-GJS-400-18 grade and castings used in wind energy. Assuming that the wind energy market accounts for 3 million tons of ductile iron per year, an estimated 30% or 900,000 tons may be suitable for SSF iron specifications. Of these, currently only 10% or 90,000 tons is produced with SSF iron.

In addition, it has been estimated that about 20% of pearlitic ductile iron produced globally could be converted to SSF iron. Currently, the global market for pearlitic ductile iron is 12.5 million tons per year. As shown in Table 1, that would mean that an estimated 2.5 million tons could be made from SSF iron based on 2018 production rates. At

Table 1. Estimated Global Annual SSF Iron Market

	Total pearlitic ductile iron	Total ductile iron
Current SSF iron market	0.25 million tons	0.34 million tons
Potential SSF iron market	2.5 million tons	3.4 million tons

this time, only 20% of this total or about 250,000 t as transitioned to SSF iron.¹¹

On an overall basis, an estimated 340,000 t per year of SSF iron is now produced globally. That means that only 1.4% of total ductile iron production of 25.5 million tons per year is SSF iron. Looking to the future, as much as 3.4 million tons per year could be made from SSF iron, based on the current ductile iron market. That would mean that an estimated 14% of the total ductile iron market could be SSF iron.

SSF Iron as a Strategic Focus

The implementation of the solution strengthened ferritic ductile iron grades into the European Standard EN 1563 in 2011 occurred at about the same time that wind turbines started to exceed 2 MW. Since the presentation at World Foundry Congress in 2000 by Björkegren,¹ there had been many encounters and questions on how to produce these high-Si ferritic ductile irons. In addition, there has been considerable discussion on the best applications for these ductile iron grades.

After the presentation by Larker at the Keith Millis Symposium in 2008, the interest in SSF iron increased substantially, and market segments such as engineering and wind energy started to look more closely at these grades. A combination of higher yield strength and elongation makes them interesting for these applications as these properties would allow for significant weight reduction in the finished casting. As the need to produce more energy per wind mill

increased, the size of the wind turbines and thus the castings used in these turbines has also increased.

With the incorporation of SSF iron into the European standard in 2011, both industry and academia recognized that not enough knowledge was publicly available about the production of SSF iron. So, while academia concentrated primarily on the chemical composition and trace elements, Elkem recognized the strategic importance of understanding how the treatment process affected the microstructure and mechanical properties.

Design of Experiments

As with non-solution strengthened ductile iron, the treatment process for SSF iron consists of a spheroidizing or nodularizing treatment followed by inoculation. Significant regional differences exist in the preferred MgFeSi treatment composition and the choice of the alloy used for ductile iron inoculation. It was therefore of interest to see if any major differences between these treatment methods significantly affected SSF iron structures and properties.

As a result, the trials were executed in the pilot test facility at Elkem Technology in Kristiansand, Norway. In these trials, the Mg treatment was made in a tundish ladle having an alloy pocket that contained the nodulizer and the cover material. The inoculant was added to the pouring ladle 1 min before pouring.

This project was divided into three sets of extensive trials, as shown in Table 2. The goal of each of the trials was to make EN-GJS-600-10 grade iron to achieve above minimum requirements for elongation, yield strength, and ultimate tensile strength. In addition, the trials sought to obtain more than 100 N/mm³ nodule density and more than 80% nodularity in a 30-mm tensile bar. This SSF grade was chosen because it would normally be difficult to achieve a good structure with restricted iron feeding. Such a structure needed to provide a high strength while balancing the carbon equivalent—also a production challenge.

Table 2. Description of Three Trials

	Trial 1	Trial 2	Trial 3
MgFeSi	A, B, C, D	A, B, E	A, E
Inoculant	1, 2, 3, 4, 5, 6, 7, 8, 9	1, 2, 3, 4	1, 3, 4
Cover	Steel	Steel + specialty FeSi	Steel + specialty FeSi
Mold	Type "a" test bar standard tensile mold	Type "a" test bar standard tensile mold + shrinkage mold	Type "a" test bar standard tensile mold + shrinkage mold

The purpose of the first trial was to see which of the preferred treatment solutions gave the best combination of mechanical properties and microstructure.

The purpose of the second trial was to verify the results from the first trial and to study the effects of cover materials, together with various combinations of MgFeSi alloys and inoculants on the microstructure and mechanical properties of EN-GJS-600-10 iron.

The purpose of the third trial was to verify results from the previous two trials and examine the effect of inoculant additions on the microstructure and mechanical properties.

The three trials had a total of four 1500-kg melts, 21 MgFeSi treatments with 5 different MgFeSi compositions, 9 different inoculants, 2 cover materials, and 2 inoculant addition rates with and without Sb. A total of 97 sets of tensile bars were produced.

The 1500-kg melts were prepared in a coreless induction furnace from ca 40% steel scrap, ca 25% pig iron, ca 30% ductile iron returns, and additives such as FeSi and a recarburizer. The target base iron composition along with typical analysis of main charge materials is shown in Table 3.

Each melt was divided into five taps of 225 kg. The melt was heated to 1550 °C for the two first trials and 1500 °C for the last trial. The tapping temperature was targeted to provide a casting temperature of 1400 ± 20 °C.

The MgFeSi addition rates were varied between 1.05 and 1.37% by weight of Mg to achieve the same target residual Mg content in the treatment ladle after deslagging. The treatment was carried out in a tundish ladle with a pocket design that allowed a 20-mm cover layer to be placed on top of the MgFeSi. After removing the tundish cover, the ladle was deslagged prior to collecting a coin for chemical analysis. The treated iron was then divided into five 32-kg

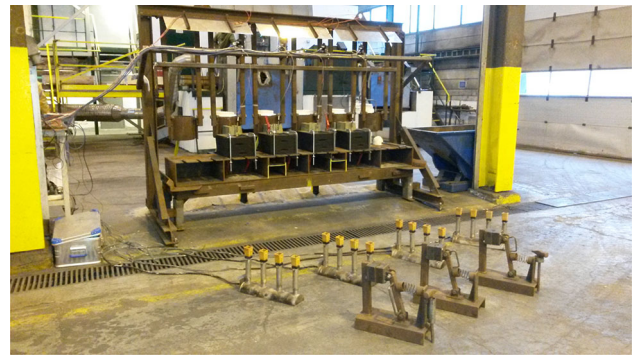


Figure 1. Test setup showing furnace ladle and pouring rig.

capacity pouring ladles at 30-second intervals. The inoculant was added to the bottom of the new pouring ladle, and the iron was then held for 1 min prior to casting into a sand mold. The same inoculant was used in the first and last pouring ladle.

The test setup is shown in Figure 1.

The type of sand mold varied from the EN 1563 separately cast option 3 round bar-shaped sample. Type “a” only standard tensile bars were used in the first trial. A combination of EN 1563 separately cast option 3 round bar-shaped samples—Type “a” and shrinkage module¹² were used in trials 2 and 3. The tensile bars and shrinkage module were built into the mold. The tensile mold, based on Norsk Standard NS-EN 1583:2001, is shown in Figure 2, while the module used to evaluate the shrinkage tendency is shown in Figure 3.

For each of the pouring ladles, a coin sample for chemical composition was collected using an immersion sampler and four thermal analysis cups were poured. The average values of the four cups were used for evaluating the inoculant performance.

The chemical composition was determined as follows:

Table 3. Target Base Iron Composition

Element	%C	%Si ^a	%S	%P	%Mn	%Ti
Target	3.20 ± 0.20	3.70 ± 0.20 3.35 ± 0.20 3.15 ± 0.20	0.012 ± 0.005	0.030 ± 0.005	Max. 0.35	Max. 0.012
Pig iron	4.10	0.15	0.005	0.024	0.03	0.02
Steel scrap	0.15	0.21	0.020	0.026	0.70 or 0.35	0.01
Returns	3.60	2.35	0.002	0.009	0.18	0.01

^aSi target was based on Si additions during treatment and the Si target needed after treatment to study the effect of Si and carbon equivalent in iron

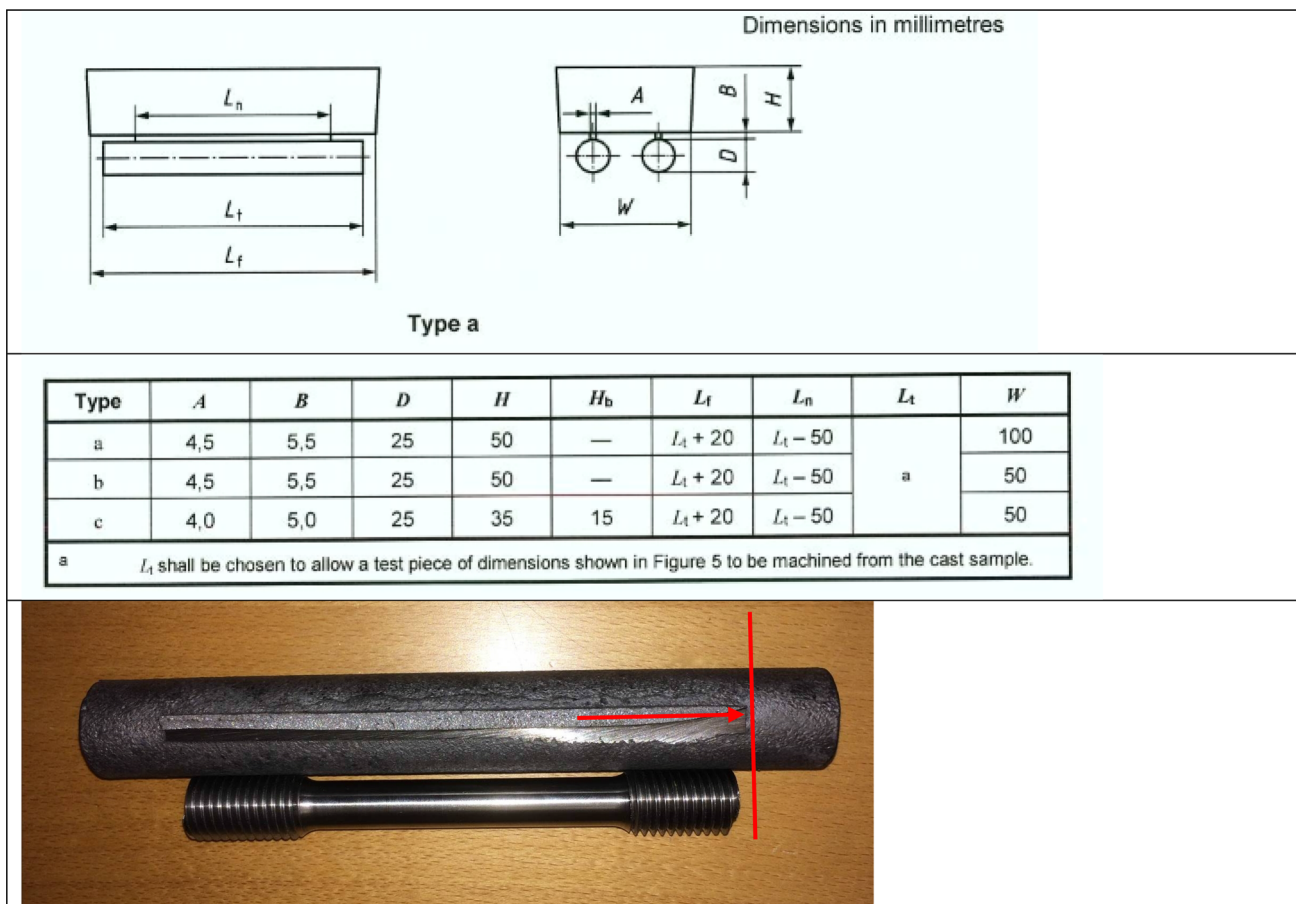


Figure 2. Tensile mold used in the trials along with an example of tensile bar prior and after machining with section used for microstructure examination indicated. The red arrow is pointing at section used for the microstructure examination.

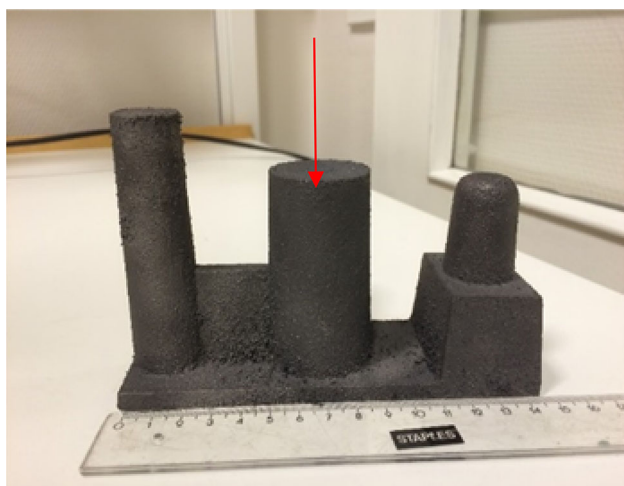


Figure 3. Shrink module used for evaluation of shrinkage tendency. The red arrow points at the section cut to evaluate shrinkage tendency.

- C and S using a combustion technique
- Si using wet chemical determination
- All other elements using an optical emission spectrometer

Each of the five 225-kg treatments took 25 min. A thermal analysis was used to monitor the melting parameters in the furnace over the 90 min the melt was held until furnace was empty. Samples were taken before each tap to check on the melt analysis.

The following parameters were used to evaluate the trials: chemical composition of the base iron, treated and inoculated iron, thermal analysis data of base iron, microstructure and mechanical properties of the final iron. A section taken from the end of one of the tensile bars was used for microstructure characterization, and both tensile bars were pulled to obtain tensile strength (R_m), yield strength ($R_{p0,2}$), and elongation (A_5).

Microstructure was determined on sample cut from the end of the tensile bar prior to machining for mechanical testing. Microstructure was determined on one of the two tensile bars poured. Microstructure quantification was carried out with a Zeiss optical microscope equipped using an Axio-plan 2 automatic stage controller at a magnification of 100 ×. The digital camera provided an image resolution of 0.68 μm/pixel (1.47 pixel/μm) and an image size of 1280 × 960 pixels. In total, 36 images were taken at

random of which 25 were manually chosen for image analysis in Image Pro Plus. The microstructure was examined in both polished (1 µm finish) and etched (Nital) conditions. Microstructure quantification was conducted on all samples except when chunky graphite was observed in the structure. Samples having chunky graphite structure were only documented with a single photograph at 100X.

Results

Chemical Composition

Since Si is the element that provides the strength in SSF iron through solution hardening of the matrix, the following correlation between Si and tensile strength has been presented by Larker:²

$$R_m = 92.9 * \%Si + 187$$

Accordingly, to achieve the target 600 MPa in ultimate tensile strength, a Si content of 4.45% would be required. No Si alternatives such as Ni, Co, or Cu were used as substitutes for Si units in these trials.

Since SSF is a cast iron, all samples contained more than 2% C. In non-solution strengthened ductile iron, the C content is normally kept as high as possible to provide the best casting properties and to minimize the shrinkage tendency. For SSF with higher Si contents, the C content must be adjusted to avoid making the C.E. too high and risking hypereutectic solidification with the formation of primary graphite.

Effect of Silicon

The final Si level varied between 4.1 and 4.5%. Based on publications by Stets,⁴ a massive drop in the statistical mechanical properties was expected at around 4.3% Si. By varying the Si level over the indicated range, this investigation hoped to see if any combination of treatment

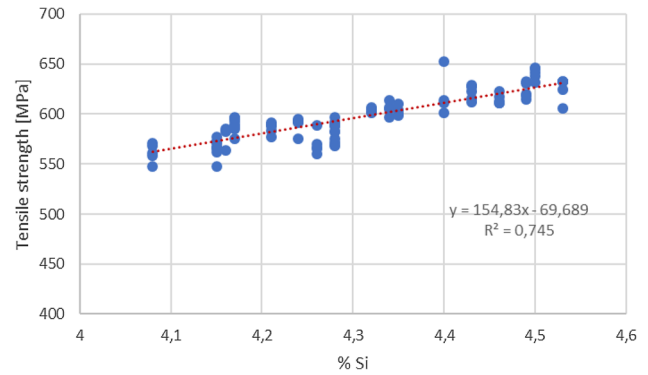


Figure 4. Tensile strength in relation to Si content.

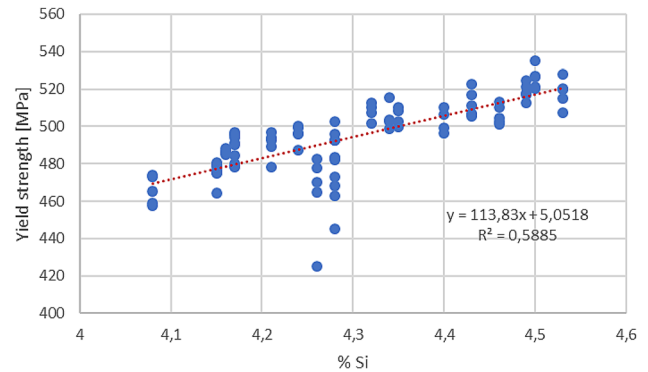


Figure 5. Yield strength versus Si content.

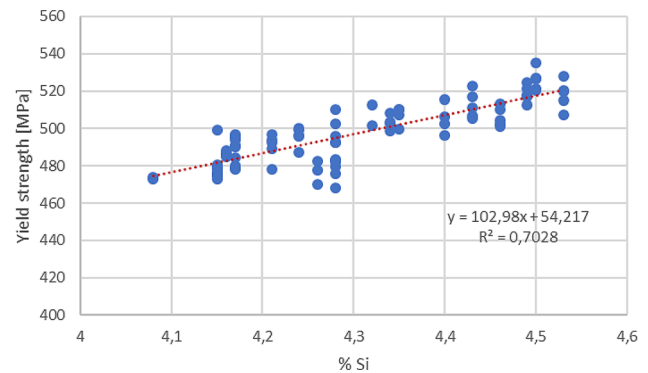


Figure 6. Yield strength versus Si content, only using the data sets points with yield strengths > 470 MPa.

Table 4. Target and Actual Final Iron Composition in the Three Trials

Element	%C	%Si ^a	%S	%Mg	%Mn	%Cu	%P	%Ti
Target	3.05 ± 0.20	4.35 ± 0.20	0.008 ± 0.005	> 0.035	0.35 ± 0.05	–	0.030 ± 0.05	Max 0.012
Actual: trial 1	2.60–2.93	4.43–4.53	0.007–0.009	0.038–0.046	0.27–0.28	0.027	0.016	0.008
Actual: trial 2	2.85–3.05	4.08–4.28	0.009–0.011	0.035–0.049	0.27–0.29	0.025	0.018	0.011
Actual: trial 3	2.75–3.08	4.29–4.30	0.011–0.013	0.040–0.046	0.32	0.017	0.025	0.003

^aC.E. = %C + 0.33 * %Si

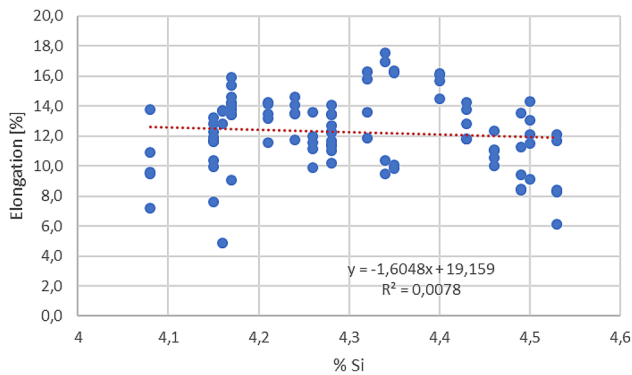


Figure 7. Elongation obtained at different Si levels.

solutions would avoid this property loss. The actual final composition ranges in the final iron are shown in Table 4.

As seen from Figure 4, the tensile strength increased with increasing Si content. According to this figure, a Si level of 4.35% would be needed to achieve the target tensile strength of 600 MPa. This is higher than the indicated turning point in the work by Stets⁴ and shows that the tensile strength continues to increase up to 4.5%. This may be due to deviation between actual and reported Si levels (See section on Si complication). The results with the highest Si level here also coincide with the lowest C, and this may have had a contributing factor in achieving the higher strength without the drop in mechanical properties. Each point in the curve is the average result of two pulled tensile bars.

A similar observation can be made for the yield strength at different Si levels, as can be seen in Figure 5.

EN-GJS-600-10 specifies that the minimum yield strength is 470 MPa. In Figure 5, all the data points have been shown, while in Figure 6, the results lower than 470 MPa yield strength have been removed because they did not meet this minimum specification. Of the total 97 sets of results, 10 were lower than 470 MPa yield strength.

Using the correlation formula between yield strength and %Si in Figure 6, a Si content of 4.0% is required to obtain the minimum yield strength of 470 MPa.

Several variables such as % C, C.E., nodule density, nodularity, and residual Mg were evaluated to study what influenced the strength. The results showed that Si is the main variable affecting both yield and tensile strength. However, % Si and matrix strength have a minimal effect on the elongation, as seen in Figure 7.

Silicon Complications

A complicating factor caused by Si is that analytical errors increase with increasing Si contents in the alloy. In

addition, there is also a lack of available CRM and RM calibration standards for SSF iron. This has also been reported by Borgstöm et al.⁸ as an issue affecting the production of SSF iron. At the Si levels required to make EN-GJS-600-10 grades, the analytical error is in the range of $\pm 0.20\%$ Si, which is equal to a potential variation in 40 MPa tensile strength. In our trials, the final Si composition was confirmed with wet chemical analysis after completion of the trials. In most of the cases, the Si level reported with optical emission spectrometer is higher than with wet chemical analysis but can also be lower. The deviation between the two methods can be as high as 0.20% Si.

Adding Si in multiple steps to achieve the Si target also becomes complicated as Si recoveries in iron vary with the processing step, the alloy used, and the sizing. To achieve the target Si and have a consistent Si recovery, it is important to include the chemical analysis of any alloys containing Si and to make sure that the chemical composition and sizing for all alloys are consistent.

Effect of Carbon

To determine the effect of carbon content, the final C level in the trials was varied from 2.6 to 3.1% and 25 microstructures were evaluated per sample. As expected in Figure 8, where each microstructure is representative of 5 similar microstructures obtained in the test, the percentage of graphite in the microstructure increased as the amount of carbon in the iron increased.

In addition, as shown in Figure 9, the tensile strength increased with decreasing C and graphite contents. Since graphite is the weak phase in an iron structure, low C contents and less graphite reduce the notch effect, strengthening the material.

At the same time, reducing the C content and the graphite can increase the shrinkage tendency in the casting, as shown in Figure 10.

As with regular ductile iron, it is important to optimize the C and Si levels in SSF iron to obtain the desired microstructure, mechanical properties, and castability.

Effect of Magnesium Ferrosilicon

Magnesium is the primary spheroidizing element used in virtually all ductile cast iron production as it is cost-effective and provides a large production window. The magnesium content of MgFeSi alloys is typically in the range of 5 to 6%. Since the recovery of Mg in iron increases with decreasing Mg levels, an increasing number

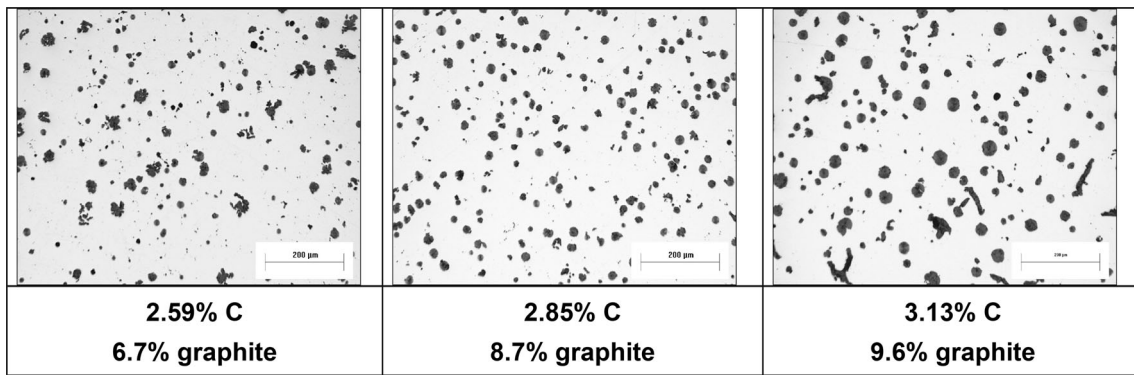


Figure 8. Percentage of graphite in the structure as the C content increased.

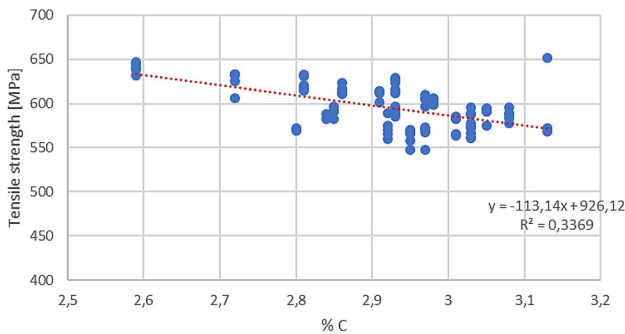


Figure 9. Effect of C content on tensile strength.

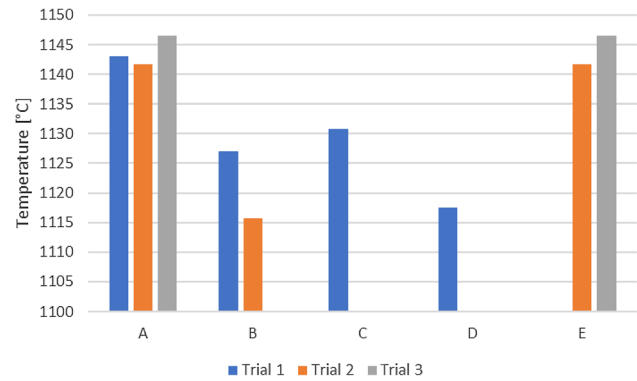


Figure 11. Difference in lower eutectic temperature observed with five different MgFeSi compositions A–E.

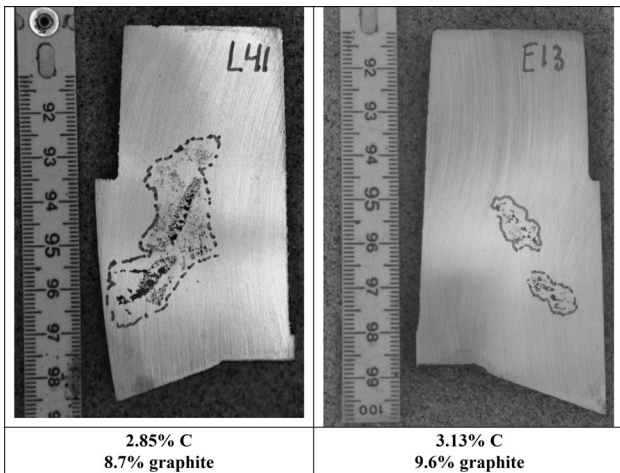


Figure 10. Effect of amount of graphite on shrinkage tendency

of foundries are using MgFeSi alloys with less than 5% magnesium.

Rare earths (R.E.) also have a long history of being part of the MgFeSi composition. However, rare earths are also believed to increase the risk of forming chunky graphite and are therefore avoided by many foundries when operating close to the eutectic or at slightly hypereutectic C.E. levels. Foundries producing larger section sizes in ferritic cast iron or high-Si irons are particularly concerned about forming chunky graphite.

Elkem's market survey also showed that there were different regional preferences for both the magnesium and rare earth contents of the MgFeSi alloys used for ductile iron treatment. Furthermore, there are differing opinions on what type of rare earth-enhanced MgFeSi is the most suitable to produce SSF iron.

Therefore, for this trial, five different MgFeSi alloys representing different regional treatment solutions were selected and ranged from 4.6 to 6% Mg and 0 to 0.5% rare earths. The type of rare earth used was also varied between materials based on misch metal and lanthanum.

Since the purpose of the Mg treatment is to tie up S and O, the number of nucleation sites is lower in ductile iron than in gray iron. For this reason, more inoculation is generally needed in ductile iron than in gray iron. One way to measure and evaluate the nucleation effect is to collect thermal analysis of samples and analyze the lower eutectic temperature. As lower eutectic temperatures are increased, foundries can expect better nucleation, requiring less inoculation later in the process.

Figure 11 shows the variation in lower eutectic temperature observed for the five different MgFeSi alloys used in the three trials. The graph shows that the lower eutectic temperature varies significantly based on the Mg content of

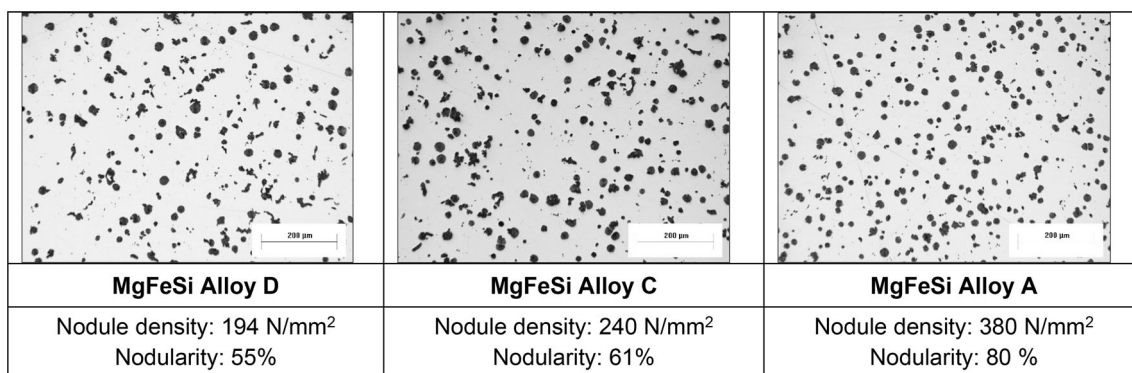


Figure 12. Difference in structure with different MgFeSi alloys using the same inoculant.

the MgFeSi alloy, with the largest increase observed when a Mg content of < 5% was used in MgFeSi treatment alloys A and E. Since the MgFeSi alloys used had different Mg levels, all additions were adjusted so that the same amount of Mg was added to the iron during each treatment. Each of these irons was inoculated with the same inoculant after the Mg treatment.

Because these MgFeSi alloys yielded different Mg recoveries, the final Mg in the iron varied between 0.038 and 0.046% in the first trial. Similarly, the final Mg varied between 0.029 and 0.041% in the second trial and between 0.040 and 0.046% in the third trial. The lowest residual Mg levels were observed in iron when MgFeSi alloys containing high Mg levels and low amounts of rare earths were used in the Mg treatment. Iron produced with these high-Mg, low R.E. alloys also had the largest Mg loss in iron between the treatment and casting processes.

Figure 12 shows the difference in nodule density and nodularity for MgFeSi alloys A, C, and D. The highest nodule density and graphite nodularity were obtained with MgFeSi alloy A, which contained <5% Mg and higher rare earths. Lower nodule densities and nodularities were obtained with MgFeSi alloys C and D, which contained high-Mg contents and low R.E. levels. A possible explanation for this is that the reaction with lower Mg is less

Table 5. Effect of Cover Materials on SSF Iron Structures and Properties

Cover type	Steel punchings (44 values)	Specialty FeSi (26 values)
Nodule density, N/mm ²	254	296
Nodularity, %	64	76
Yield strength, MPa	478	496
Tensile strength, MPa	577	590
Elongation, %	12	14

violent than with higher Mg-containing MgFeSi, and thus, more inclusions are left in the iron to facilitate easier nucleation of graphite later. This also explains why a higher Mg yield is seen with MgFeSi with lower Mg contents than with MgFeSi containing higher Mg contents.

Effect of Cover Material

The main reason to use a cover material is to delay the MgFeSi alloy from reacting with the liquid iron while iron

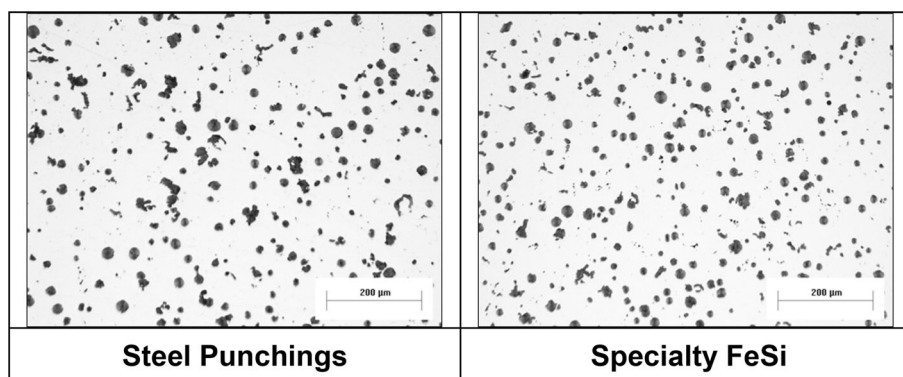


Figure 13. Difference in nodularity due to different cover materials but the same MgFeSi alloy and inoculant.

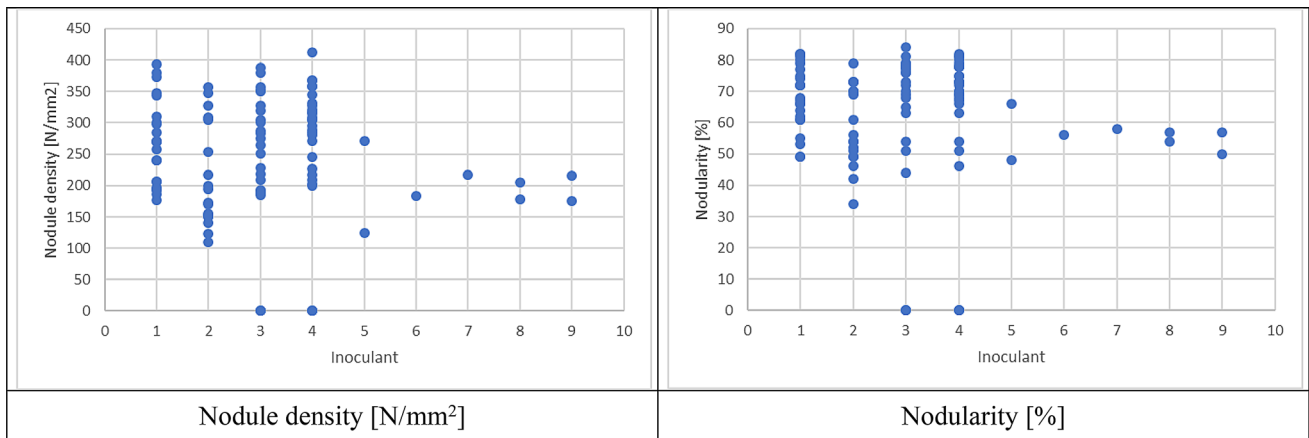


Figure 14. Variation in nodule density and nodularity for different inoculant types tested.

Table 6. Effect of Inoculants on SSF Iron Structures and Properties

	Inoculant 1 Ca + Al	Inoculant 2 Ca + Al + Ba	Inoculant 3 Ca + Ce	Inoculant 4 Ca + Ce + Bi
Nodule density, N/mm ²	271	200	304	304
Nodularity, %	82	70	84	82
Yield strength, MPa	491	490	496	494
Tensile strength, MPa	588	585	597	593
Elongation, %	15.4	13.5	16.0	14.6

is filling the ladle. This increases the amount of liquid metal above the alloy before the reaction starts.

The type and composition of the cover material often vary from foundry to foundry. In these trials, dry steel punchings having a defined size were compared to a specialty FeSi alloy having a defined composition and size. The Si content of the cover addition was the same for both practices, since high-purity Si was added with the steel punchings to equalize the Si addition. This insured that Si did not affect the results.

Figure 13 and Table 5 show that regardless of the MgFeSi alloy used, the specialty FeSi cover provided significant improvements in nodule density, nodularity, yield strength,

tensile strength, and elongation. It is believed that in addition to delaying the reaction an inoculating effect is also obtained from the specialty FeSi cover and results in improved graphite structure and consequently improved mechanical properties.

Effect of Inoculation

Both the type of the inoculant and its addition rate can influence the final graphite structure and the mechanical properties of SSF iron. In these trials, various inoculant types were tested in combination with different iron compositions, MgFeSi alloys, and cover materials. The types of inoculants used consisted of Sr + Zr (5), Ca + Ba (2),

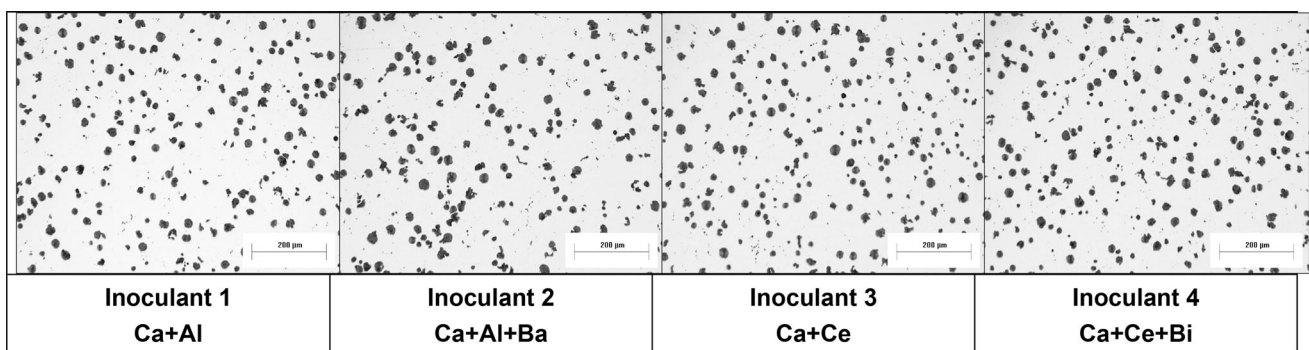


Figure 15. Variation in graphite structure for different types of inoculants under similar production conditions.

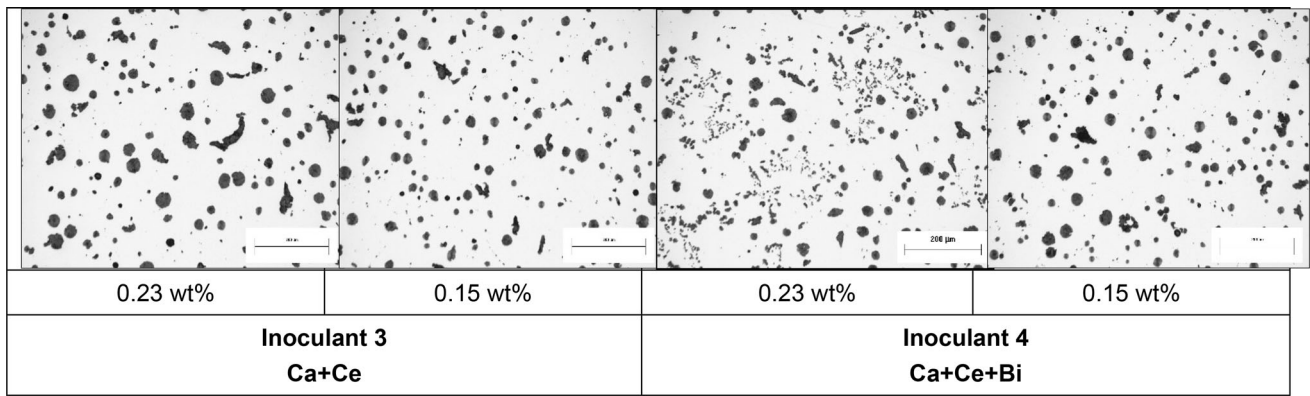


Figure 16. Improved graphite structure from reduced late-stage inoculation addition.

Ca + Al (1, 6), Ca + Ce (3, 8), Ca + Ce + Bi (4), and Ca + Al + Zr (7, 9) inoculants.

Different inoculants gave variations in nodule density and nodularity, but the variation between the inoculants was overpowered by the iron composition, MgFeSi quality, and cover type, as seen in Figure 14.

Figure 15 and Table 6 show the typical graphite structure obtained with four different inoculants using the same Mg treatment. For three of the inoculants, there is very little visual difference and no significant difference in nodule

density and nodularity. However, the structure formed by inoculant 2 has significantly less nodule density and nodularity. The differences between the inoculants were 104 N/mm² nodule density, 12% nodularity, 2.5% elongation A₅, 6 MPa yield strength R_{p0.2}, and 12 MPa tensile strength.

The type of inoculant used was therefore not found to be significant in these trials, and all the inoculant types tested provided acceptable microstructures.

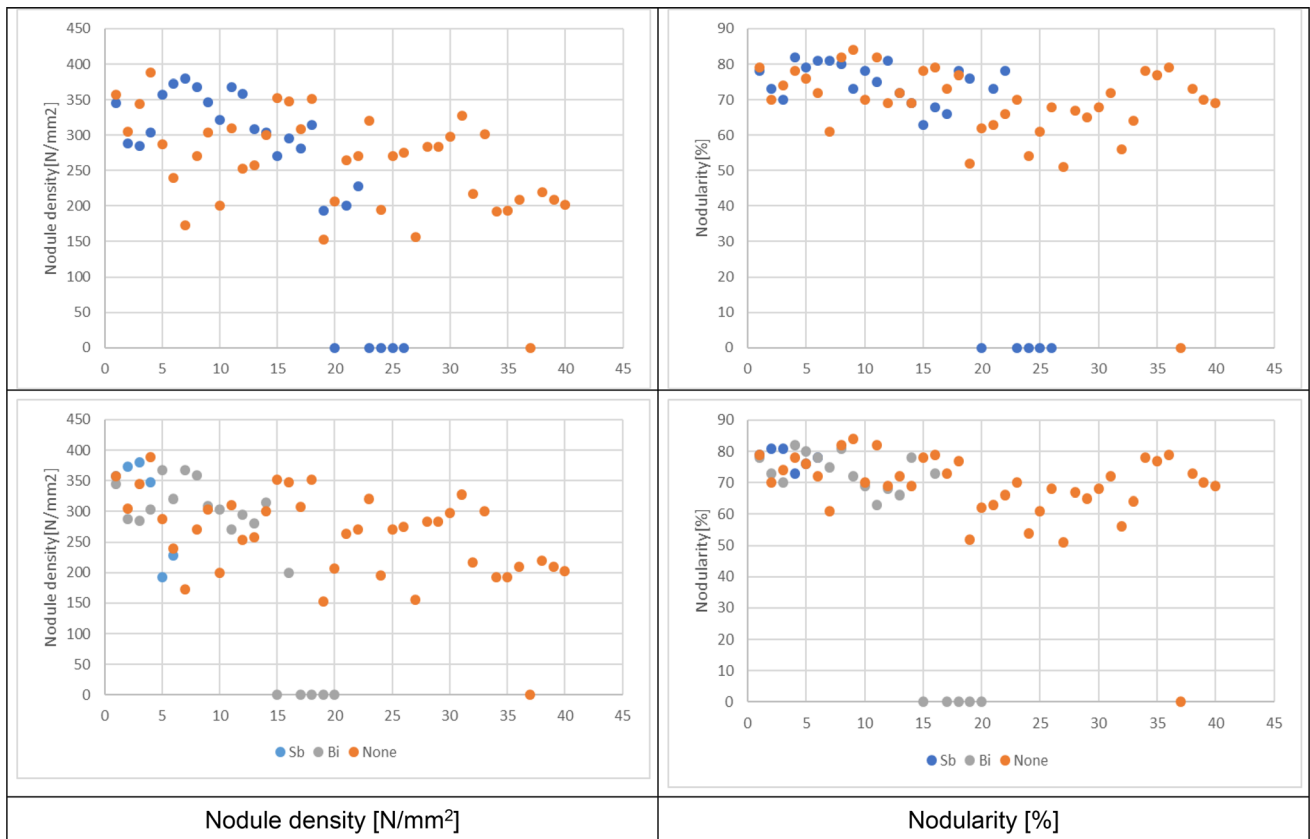


Figure 17. Comparison of nodule density and nodularity for samples treated with Sb or Bi (blue dots) versus samples without treatment with Bi or Sb (orange dots).

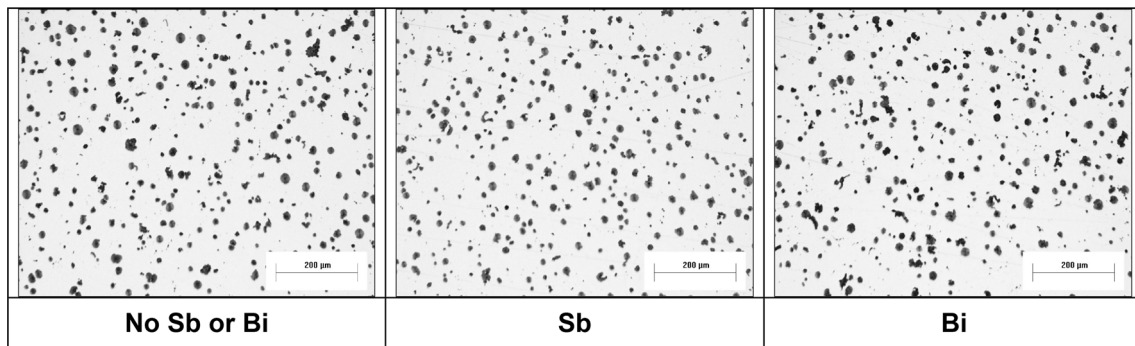


Figure 18. Nodule density and nodularity of samples treated with Sb or Bi compared to a sample without either of these two elements.

Figure 16 shows that in Trial 3, it was observed that regardless of the type of inoculant used in iron having the highest Si levels, a reduction in the inoculation addition actually improved the structure.

Effect of Antimony and Bismuth on Inoculation

Antimony (Sb) additions in the range of 20–100 ppm are frequently used to counteract chunky graphite and improve nodule density in fully ferritic, heavy ductile iron castings. The addition of Sb is based on the section size and Ce level of the iron. Furthermore, the use of inoculants with Bi + R.E. has been reported to be very successful in controlling chunky graphite in SSF iron by Stets and Löblich.⁴

In these trials, Sb and Bi were tested to see if either of these elements had any significant effect on the graphite structure at a given section size. To test Sb, a separate 20-ppm Sb addition was made to iron without Bi + R.E. inoculation. Then, a Bi + R.E. inoculant with a 1:1 R.E.-to-Bi ratio was tested without a Sb addition. The graphite structures formed by these two practices were then compared to iron structures that had no Sb or Bi treatment.

In Figure 17, the nodule density and nodularity are shown for the Sb- or Bi-treated iron and compared to the iron where no Sb or Bi was added. While Sb or Bi might have some positive effect on the nodule density, there was no

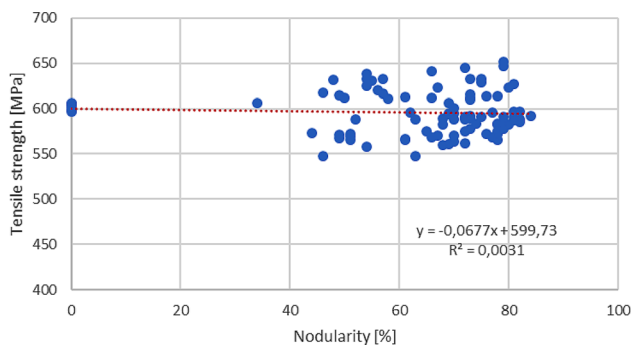


Figure 19. Effect of nodularity on tensile strength.

significant effect on the nodularity. In fact, the six samples having no nodularity or nodule density (5 blue dots and 1 orange) had chunky graphite in their microstructures.

In Figure 18, the structure of iron treated with Sb and Bi was compared to the structure of iron not treated with these two elements. Both irons were nodulized with the same MFeSi alloy and cover material. The microstructures show that neither Sb nor Bi had any significant effect on the graphite nodules. In fact, Bi substantially increased the amount of chunky graphite in the sample with the highest Si level.

Effect of Graphite Structure

The ISO standard for SSF ductile iron acknowledges that SSF iron with higher Si levels is more prone to degenerated graphite as it approaches the hypereutectic composition needed to obtain the required strength, the best castability, and the lowest shrinkage tendency. This graphite risk is probably related to the possible formation of graphite early in solidification where it can grow over time in liquid iron.

This highest risk of forming degenerated graphite in SSF iron, especially in EN-GJS-600-10 grades, takes place in structures with overall low nodularity and chunky graphite compared to normal ductile iron. However, since SSF iron is a single matrix material, the matrix controls the strength

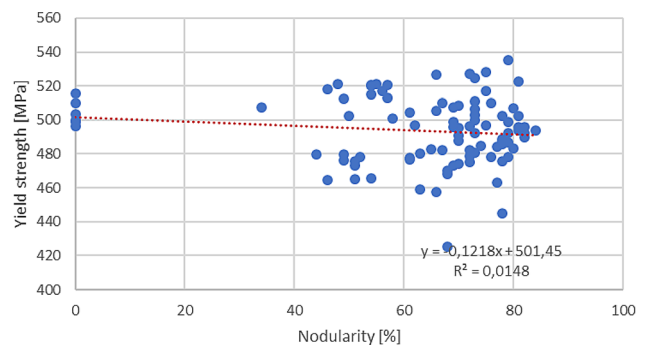


Figure 20. Effect of nodularity on yield strength.

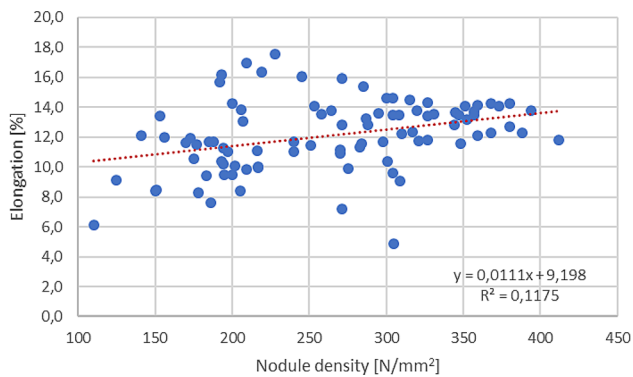


Figure 21. Effect of nodule density on elongation.

of the iron and reduces section sensitivity. By avoiding low nodularity in SSF iron, foundries can optimize strength properties.

Ultimate Tensile Strength

Figure 19 shows that the nodularity of SSF iron has a limited effect on ultimate tensile strength. For samples where chunky graphite was found in the structure and not quantified, the nodularity was set at 0. In six cases, chunky graphite was found in the structure of samples taken from a 30-mm tensile bar. These 6 points can be seen on the left of this graph, and all points are shown to have a tensile strength of 600 MPa. As a result, the low nodularity of SSF iron appears to have less impact on the ultimate tensile strength than on samples of non-solution strengthened ductile iron.

Yield Strength

Figure 20 shows that the variation in yield strength is generally greater over the nodularity range observed in the trials as well as for the samples where chunky was graphite present in the structure. However, a minimum of 400 MPa yield strength was still obtained in the samples with chunky graphite. There were also more individual samples with a

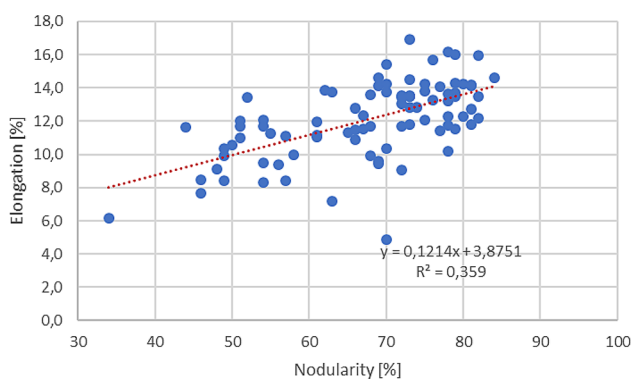


Figure 22. Effect of nodularity on elongation.

lower yield strength at a nodularity of > 60% than at a nodularity of around 50%. Based on these results, a low nodularity has less impact of the yield strength of SSF iron than it does on non-solution strengthened ductile iron.

Elongation

While the Si content and the matrix have a major influence on the tensile and yield strength of SSF iron, the graphite structure strongly affects the elongation, as seen in Figures 21 and 22.

Figure 21 shows that the % elongation increases as the nodule density increases, with the highest elongation values being obtained for nodule densities in the range of 200–250 nodules/mm². In Figure 22, the same samples have the highest nodularity, indicating that the shape of the nodules is more important than the number of nodules. However, a high nodule density is often associated with a high nodularity.

In addition, the nodularity of graphite appears to have a greater influence on elongation than nodule density. In fact, a nodularity of around 50% provides an elongation of 10%. The round graphite nodules also lower the notch effect and increase their ability to reduce stress concentration in front of a growing crack.

In Figure 23, examples of structures and their elongation values are shown in 30-mm tensile bars having a nodularity ranging from 50 to 80%. While the chemical composition, specifically Si, controls the matrix, the shape of the nodules controls the elongation. Because of its strong matrix, however, SSF iron can tolerate more degenerated or poorly shaped graphite nodules than non-solution strengthened ductile iron.

Summary: A Promising Future

Solution strengthened ferritic ductile iron (SSF) was originally developed as a substitute for standard ferritic–pearlitic ductile iron used in automotive applications. The interest in this iron was sparked by its more uniform hardness and lower machining costs due to the single matrix in the iron. Today, however, the wind energy market is pushing this material forward because designers are interested in the material’s higher yield strength and elongation—a combination that can allow considerable weight reduction in the finished casting.

The main hurdle facing SSF iron is that it is a brittle material due to its elevated Si levels. This issue is being addressed through greater technical understanding of the material, more accurate testing methods, and realistic test conditions that consistently provide the properties which

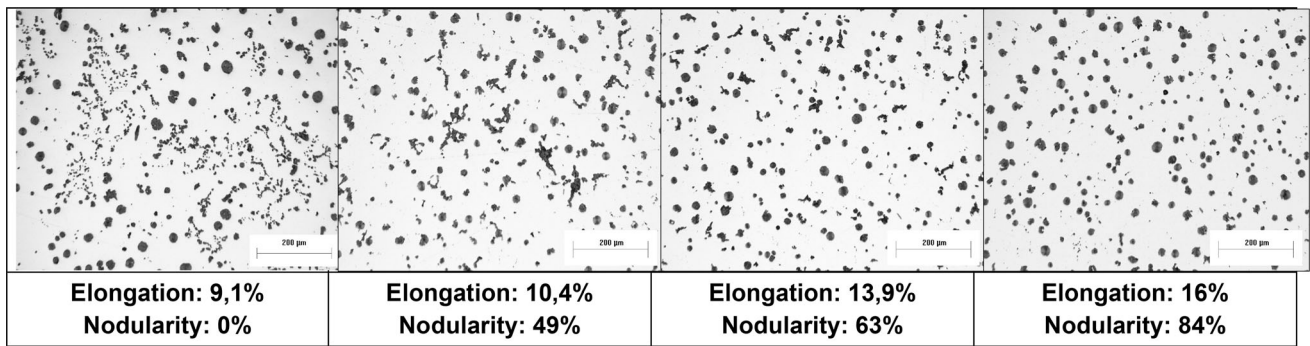


Figure 23. Examples of SSF iron microstructures with corresponding elongation values.

designers and engineers need to obtain a potential weight reduction. Data related to fracture toughness and crack-growth behavior are now being requested instead of Charpy impact values. Recently, additional testing has revealed the property advantages and limitations for SSF iron, allowing designers to select this material for specific applications with greater confidence.

The Si level in SSF iron is the key parameter that controls the strength, while the graphite structure—especially the shape of the graphite—controls the elongation. In addition, C is needed to get sufficient graphite to control the shrinkage tendency. As in standard ductile iron, Si, C, and thus the carbon equivalent needs to be adjusted to get the best castability and lowest shrinkage tendency. The elevated Si level also increases the risk of chunky graphite formation, especially in the SSF grade EN-GJS-600-10 with its highest strength and Si level.

This study showed that the treatment process using a combination of different MgFeSi alloys and cover materials had a more significant impact on the structure and properties of SSF iron than the choice of the inoculant. In fact, various MgFeSi alloys and cover materials were found to result in up to 50% higher nodule density and graphite nodularity, regardless of the type of inoculant used. In fact, SSF iron with the highest Si levels actually had the highest risk of forming the chunky graphite that reduces iron properties.

In addition, in the section size tested, no significant structural differences could be observed between Sb + R.E., Bi + R.E., and non-Sb/Bi treatments. While some improvement in nodule density was found, the nodularity was in most cases not improved.

Although more degenerated graphite can be found in SSF iron than in standard ductile iron, nodularities as low as 50% can be tolerated in the structure without negatively affecting static mechanical properties such as elongation, yield strength, and tensile strength. Working with high-Si ductile iron like SSF iron also provides an added challenge because of the difficulty in accurately measuring high-Si

levels, possibly impacting the results. The same concerns apply to Si-containing raw materials, where a consistent chemical analysis and sizing are needed to control Si additions and yields.

Like standard ductile iron, there are many ways to produce SSF iron successfully. However, this study shows that various combinations of MgFeSi alloys, cover materials, and inoculants allow foundries to safely and consistently obtain the required properties needed for SSF iron to reach its ultimate potential.

Acknowledgements

The authors would like to thank John Crane for his extensive efforts and assistance with editing the paper and Bente Kroka for her contribution and help with evaluating the microstructure and shrinkage tendency.

REFERENCES

1. L.E. Björkegren, K. Hamberg, Silicon alloyed ductile iron with excellent ductility and machinability. *Keith Millis Symposium*, 2003
2. R. Larker, Solution strengthened ferritic ductile iron ISO 1083/JS/500-10 provides superior consistent properties in hydraulic rotators. *Keith Millis Symposium*, 2008
3. Meghan Oaks, “Letting Mr. Charpy Die”. *DIS Conference*, 2011
4. W. Stets, Solution strengthened ferritic ductile cast iron according DIN EN 1563: 2012-properties, production and application. *Keith Millis Symposium*, 2013
5. S. Değirmenci, B. Şirin, B. Duit, EN 1563—new generation ductile irons. *7th International Istanbul Foundry Congress*, 2014
6. R. Okunnu, High strength solution-strengthened ferritic ductile cast iron. Master Thesis, 2015
7. R. Logan, C. Hartung, Solution strengthened ferritic iron DIS survey. *DIS Conference*, 2016
8. P. Hammersberg, K. Hamberg, H. Borgström, J. Lindkvist, L.-E. Björkegren, Modelling the variation

- of tensile properties of high silicon ductile iron. *AFS 2018 Metalcasting Congress*
9. J. Scrunton, P. Sanders, MTU, DIS, Research Project Proposal, Solid solution strengthened ferritic ductile iron (SSFDI) effects and limitations of residual alloying elements. *DIS Meeting Minutes*
 10. Modern Casting Staff Report, Census of world casting production - global casting production growth stalls. *Mod. Cast.* **107**(12), 24–28 (2017)
 11. Internal Elkem Estimates for Current and Future Markets for SSF Iron
 12. N. Tenaglia, R. Boeri, G. Rivera, J. Massone, Study of shrinkage porosity in spheroidal graphite cast iron. *Int. J. Cast. Metal. Res.* **29**, 112–120 (2016)

Publisher's Note Springer Nature remains neutral with regard to jurisdictional claims in published maps and institutional affiliations.